

Topological singularity-induced self-energy in strongly correlated fermion systems

Byungkyun Kang,^{1,*} Zachary Brown,² Myoung-Hwan Kim,² Hyunsoo Kim,³ and Chul Hong Park⁴

¹College of Arts and Sciences, University of Delaware, Newark, Delaware 19716, USA

²Department of Physics and Astronomy, Texas Tech University, Lubbock, Texas 79409, USA

³Department of Physics, Missouri University of Science and Technology, Rolla, 65409, MO, USA

⁴Quantum Matter Core-Facility and Research Center of Dielectric and Advanced Matter Physics, Pusan National University, Busan 46240, Republic of Korea

Employing ab initio many-body perturbation theory combined with dynamical mean field theory, we discovered that in strongly correlated topological semimetals HoPtBi and PrAlGe, which exhibit topological singular points in the vicinity of the Fermi level, the formation of $4f$ quasiparticles are forbidden. We show that blocking hybridization channels at the topological singular point effectively enhances on-site Coulomb repulsion, resulting in a substantial self-energy. This renders the topological singular point incompatible with the presence of strongly correlated electrons at the Fermi level. In contrast to the Kondo effect, our findings suggest that the topological quasiparticles in close proximity to the singular points do not hybridize with $4f$ electrons due to the self-energy, thus hindering the manifestation of heavy-fermion behavior when the singular points persist at the Fermi level.

Introduction. In condensed matter, electrons at the Fermi energy (E_F) preside over the majority of intriguing physics. In strongly correlated electron systems, the presence of a moderate Coulomb repulsion can give rise to the emergence of Fermi-liquid quasiparticles at low-energy scales. These excitations occur through the creation of screening holes, which effectively reduce the strength of the Coulomb repulsion U_C (Fig. 1a). The strongly correlated $4f$ electrons of rare-earth elements (R- $4f$) are capable of accommodating a quasiparticle state at E_F . At low temperatures, the Nd- $4f$ electrons in superconducting nickelate NdNiO₂ induce a quasiparticle with Kondo hybridization, resulting in a three-dimensional Fermi surface, which is responsible for the inconsistent superconductivity observed in nickelate superconductors [1]. The band-dependent quasiparticle dispersion around E_F of the Ce- $4f$ in the heavy-fermion superconductor CeCu₂Si₂ has been observed, lending credence to the $d+d$ pairing scenario for unconventional superconductors [2]. The hybridization of Pr- $4f$ electrons with conduction electrons in filled-skutterudite PrRu₄P₁₂ has been observed to result in anomalous behaviors, the most notable of which is a giant negative magnetoresistance [3].

In topological semimetals, the emergence of topological quasiparticles in the immediate vicinity of Weyl points or quadratic band touchings gives rise to intriguing and unconventional physical phenomena. The rare-earth elements present in the attractive Weyl semimetals RAlGe (R=rare-earth) have been suggested to be associated with the exotic electronic properties [4–12]. These include high Fermi velocities [10], Lorentz-violating type II Weyl fermions [6] in LaAlGe, a strong anomalous Hall effect in the ferromagnetic Weyl semimetal PrAlGe [7, 11, 12], and a topological magnetic phase in CeAlGe [8]. A recent study suggested that the formation of defects in LaAlGe can significantly alter the chemical potential, thereby impacting these unique electronic characteristics resulting from Weyl physics [13]. The

rare-earth elements are of paramount importance in topological half-Heusler compounds. The tuning of R- $4f$ electron in topological semimetals RPdBi provides a distinct opportunity to modulate the strength of magnetic interaction, thereby enabling a precise adjustment of the normal-state band inversion strength, superconducting pairing, and magnetically ordered ground states [14]. The antiferromagnetic Weyl semimetal compounds GdPtBi and NdPtBi [15], as well as the topological semimetal HoPtBi [16], have been observed to exhibit an anomalous Hall effect.

Recently, experimental studies on the unusual behavior of Berry curvature in Kondo lattices have been reported [17–19], along with theoretical investigations on the breakdown of topological invariants in strongly correlated systems [20]. These findings highlight the influence of strongly correlated electrons on the topological state. However, precise nature of the interplay between quasiparticles originating from strongly correlated fermions and topological singular points remains elusive. The conundrum of rare-earth-based topological semimetals lies in their possession of both strongly correlated $4f$ electrons and topological singular point. The most intriguing physical phenomenon occurs when E_F is precisely situated at the topological singular point of Weyl cones and quadratic bands. At low temperatures, therefore, the emergence of R- $4f$ quasiparticles in semimetals could result in a dramatic alteration of their physical properties. In this study, we present our findings on the impact of topological singular points at E_F on the formation of $4f$ quasiparticles, which is impeded by their interference with the essential hybridization channel (see Fig. 1b). In topological semimetals of HoPtBi and PrAlGe, the $4f$ quasiparticle is pushed away from E_F due to the effective Coulomb repulsion U_{eff} . This repulsion is intensified from U_C by the diminished screening effect caused by the highly reduced hybridization with the robust topological singular point at E_F (see Fig. 1c).

Topological singularity-induced self-energy. The linearized quasi-particle self-consistent GW + dynamical mean field theory (LQSGW+DMFT) method [21] was utilized in order to conduct an analysis of the electronic structure of rare-earth-based topological semimetals. Simulations of HoPtBi re-

* bkang@udel.edu

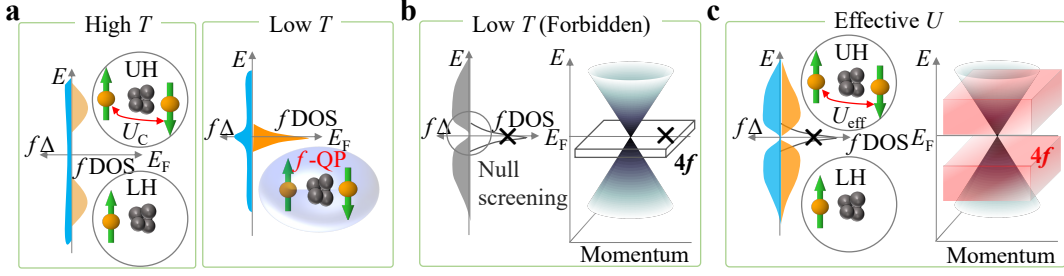


FIG. 1. **Schematic diagram of exclusive interplay between $4f$ quasiparticle and topological singular point.** **a**, In general, a strongly correlated electron can be in a Mott phase with an upper Hubbard band (UH) and lower Hubbard band (LH) at high temperatures due to the Coulomb repulsion (U_C). The emergence of $4f$ quasiparticle (f -QP) occurs in the presence of a weak U_C at low temperatures, where the U_C is screened by $4f$ hybridization (Δ) with neighboring orbitals. **b**, In $4f$ -based topological semimetals, the $4f$ Δ is primarily influenced by the density of states (DOS) of the topological bands. The topological singular point (t-SP) at the Fermi level (E_F) does not provide the necessary hybridization environment for the formation of f -QP, since the DOS at the t-SP energy is diminished. As a result, the formation of f -QP at E_F is hindered. **c**, In the HoPtBi and PrAlGe, the t-SP is formed at E_F . As a result, the DOS at E_F is subtle, and the t-SP does not provide a hybridization environment for the formation of f -QP. The absence of screening leads to a strong effective Coulomb interaction (U_{eff}), which in turn gives rise to the formation of lower (LH) and upper (UH) Hubbard-like $4f$ bands.

TABLE I. The electron occupation of Rare Earth- $4f$ orbitals and the Z factor were calculated. The Z factor was presented only when it was greater than zero. The $4f$ orbitals are labelled for convenience in this work.

j	4f occupancy (Z factor)														
	5/2						7/2								
j_z	-2.5	-1.5	-0.5	0.5	1.5	2.5	-3.5	-2.5	-1.5	-0.5	0.5	1.5	2.5	3.5	
label	f_1	f_2	f_3	f_4	f_5	f_6	f_7	f_8	f_9	f_{10}	f_{11}	f_{12}	f_{13}	f_{14}	
HoPtBi	T=100 K	0.98 (0.51)	0.98 (0.55)	0.98 (0.59)	0.98 (0.58)	0.98 (0.55)	0.98 (0.56)	0.54 (0.04)	0.52 (0.03)	0.53 (0.03)	0.50 (0.02)	0.51 (0.02)	0.47 (0.01)	0.48 (0.01)	0.47 (0.01)
	T=300 K	0.97 (0.36)	0.96 (0.67)	0.96 (0.41)	0.97 (0.38)	0.97 (0.32)	0.97 (0.43)	0.52 (0.03)	0.52 (0.03)	0.51 (0.03)	0.48 (0.02)	0.56 (0.04)	0.51 (0.03)	0.51 (0.03)	0.51 (0.03)
PrAlGe	T=100 K	0.43 (0.11)	0.42 (0.13)	0.01 (0.13)	0.01 (0.13)	0.42 (0.13)	0.44 (0.12)	0.01	0.01	0.01	0.00	0.00	0.01	0.01	0.01
	T=300 K	0.38 (0.12)	0.37 (0.13)	0.16	0.16	0.36 (0.13)	0.38 (0.12)	0.01	0.01	0.01	0.01	0.01	0.01	0.01	0.01

vealed a distinct self-energy form, exhibiting a pronounced correlation between $4f$ quasiparticle and topological singular point. Fig. 2a shows a topological singular point at the Γ point at E_F , while the Ho- $4f$ orbitals projected spectral weight is prohibited at E_F , as shown in Fig. S8. Table I and Fig. S7 demonstrate that the six f orbitals in the $f_{5/2}$ multiplet are completely filled and exhibit similar behavior, while the eight f orbitals in the $f_{7/2}$ multiplet are partially filled. Fig. 2b illustrates that the DOS for Ho- f_{10} , which is representative of the $f_{7/2}$ multiplet, is zero at E_F .

The quasiparticle weight Z was calculated and is presented in Table I. This value was determined by the gradient of the imaginary component of the self-energy, $Z = 1/(1 - \frac{\partial \text{Im}\Sigma(i\omega)}{\partial i\omega})|_{i\omega \rightarrow 0^+}$. The increase in mass caused by electronic correlations can be calculated as the inverse of the quasiparticle weight, $\frac{m^*}{m} = \frac{1}{Z}$ [22]. The Z factor is of interest, as it ranges from 1 for weak electron correlation to 0 for strong electron correlation [23]. As shown in Fig. 2b and Fig. S6, the topological singular point remains at E_F upon cooling. Whereas Mott-like physics with strong self-energy is diminishing as lowering temperature in general [1], the self-energy

of Ho- $4f$ in the real axis remains strong. The calculated Z factor remains at ~ 0.03 in the temperature range, indicating that strong correlation persists, pushing the f DOS away from E_F and maintaining the topological singular point at E_F at low temperature. This indicates that the self-energy of Ho- $4f$ appears to remain relatively unaffected by the Mott-like physics solely attributed to U_C , as evident from the modest static U_C of 2.03 eV for Ho- $4f$ (Fig. S2). The $4f$ quasiparticle is strongly correlated with the topological singular point, which is responsible for the majority of the self-energy of Ho- $4f$ in HoPtBi.

Enhanced Coulomb repulsion through null screening. Examining the local angular momentum correlation functions $\chi_{J_z}(\tau) = \langle J_z(\tau)J_z(0) \rangle$ for HoPtBi and PrAlGe, as depicted in Fig. 2c, provides insight into the degree of magnetic moment localization [24]. The $\chi_{J_z}(\tau)$ of both semimetals exhibit a small reduction as the τ increases, implying the presence of substantial local magnetic moments. The almost flat $\chi_{J_z}(\tau)$ of R- $4f$ is consistent with that of the transition metal- d in the Mott phase of NiO and FeSe [25, 26], indicating that the behavior of R- $4f$ electrons in these semimetals can be elucidated through the lens of local atomic characteristics, where

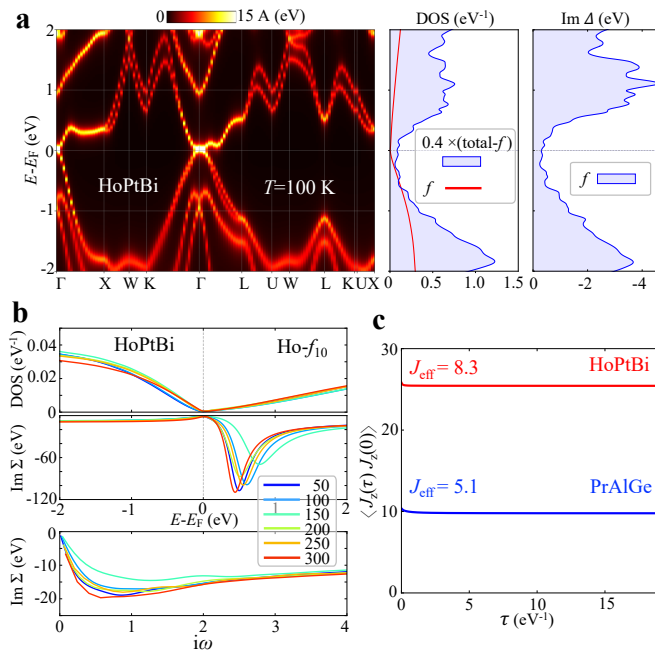


FIG. 2. **Effect of temperature on the electronic structure of HoPtBi.** **a**, Spectral functions of HoPtBi at $T=100$ K (left panel), projected DOS of Ho-4f and the total DOS with the Ho-4f component subtracted (middle panel), and the imaginary part of the hybridization function (Δ) of Ho-4f. **b**, f_{10} projected DOS, imaginary part of self-energies on the real frequency axis and on the imaginary frequency axis of HoPtBi, at varying temperature in unit of Kelvin. **c**, Local angular momentum correlation functions in the imaginary time τ for HoPtBi, PrPtBi, and PrAlGe. Calculated instantaneous J are presented with corresponding colors.

the on-site Coulomb interaction plays a significant role. Fig. S2 shows the dynamical on-site Coulomb interaction U_C . In HoPtBi, a small static U_C for Ho-4f exerts a significant local screening effect on the local dynamics, ultimately enhancing the probability of 4f quasiparticle formation, as schematically shown in Fig. 1a. The pronounced frequency dependence of U_C for Ho-4f within the low-frequency range suggests the presence of a narrow and distinct 4f quasiparticle peak at E_F [27]. However, as shown in Fig. 2a, the DOS of neighboring orbitals in the vicinity of the Fermi level approaches zero as a result of the formation of the topological singular point. This leads to a substantial reduction in 4f hybridization functions, that present the extent to which 4f orbitals are mixed with adjacent orbitals, and consequently, the shielding of the 4f Coulomb repulsion [28]. Hence, the 4f quasiparticle located at E_F is exposed to negligible screening and undergoes a significant effective Coulomb interaction U_{eff} leading to a Mott-like phase transition (see Fig. 1c). As shown in Fig. 2b, this exclusive interplay resulted in a decrease in self-energy at temperatures from 300 to 150 K due to the weakening of Mottness and an increase in self-energy at temperatures from 150 to 50 K due to the enhanced null screening effect caused by a higher probability of 4f quasiparticles at lower temperatures. This effect was also reflected in the half-filling occupancy (Ta-

ble I) and the emergence of a Mott-like characteristic in both the upper and lower Hubbard-like bands (Fig. S7).

Incompatibility between the 4f quasiparticle and the topological singular point at E_F . We have demonstrated a unique interaction between 4f electrons and topological singular point arising from quadratic bands touching. In order to further investigate this interaction with other types of topological singular point, we have conducted a study on PrAlGe, a semimetal with topological singular point originating from linear band crossing near the Fermi level. As shown in Fig. 3b and Fig. S3, the spectral function of LaAlGe closely resembles the LQSGW bands, which exhibit a renormalization of the DFT bands. This suggests that there is not a significant level of strong correlation in LaAlGe, as it does not contain 4f electrons. Nevertheless, when the correlated Pr-4f electrons in PrAlGe are treated within the DMFT approach, there is a modification to the band structure, particularly near the Γ point, as depicted in Fig. S3, compared to the results obtained from DFT and LQSGW methods. In Fig. 3c, both the Fermi surfaces of LaAlGe and PrAlGe are in agreement with the ones that were measured [6, 12], and there is a significant contrast between the Fermi surface of LaAlGe and that of PrAlGe. These findings suggest that the Pr-4f electrons are located near E_F , which has a significant impact on the electronic configuration of PrAlGe.

Fig. 3a presents the spectral functions and DOS of PrAlGe at simulation temperatures of 100, 200, and 300 K. At 300 K, a flat Pr-4f band is observed at ~ -0.3 eV. As the temperature decreases, this band gradually moves closer to E_F , centering at ~ -0.2 eV at 100 K. At a low temperature, the Pr-4f band exhibits a more coherent character, which is evidenced by its brighter, narrower, and two-peak structure, in conjunction with adjacent orbitals at 100 K. The evolution of the Pr-4f quasiparticle has a profound impact on the shape of topological singular points. At the Σ high-symmetry point, the emergence of Weyl node W1 has been reported in previous studies [4, 6]. As the temperature decreases, it is noted that the two intersecting points positioned just above E_F exhibit a closer proximity. The Pr-4f quasiparticle is responsible for the observed effect, as indicated by the unaltered state of the corresponding nodes in LaAlGe across the same range of temperatures, as illustrated in Fig. S4. However, the Pr-4f quasiparticle did not affect the energy level of the topological singular point.

The Pr-4f orbital-resolved DOS and self-energy are shown in Fig. 3d and e. As the temperature decreases, there is an increase in the DOS for f_2 , and its peak position shifts towards E_F , manifesting a tendency to converge at ~ -0.2 eV. Of greater significance is the fact that the f_2 DOS is suppressed at E_F across all temperature ranges. The quasiparticle peak is augmented as the temperature is lowered, due to a decrease in the self-energy, as demonstrated by the imaginary part of the self-energy in Fig. 3d. As illustrated in the inset of the imaginary self-energy on the real axis, similar to the f_2 DOS, the self-energy shows a tendency to converge below 150 K. This suggests that the enduring self-energy at lower temperatures is derived from U_{eff} , which is amplified when the 4f quasiparticle approaches the topological singular point.

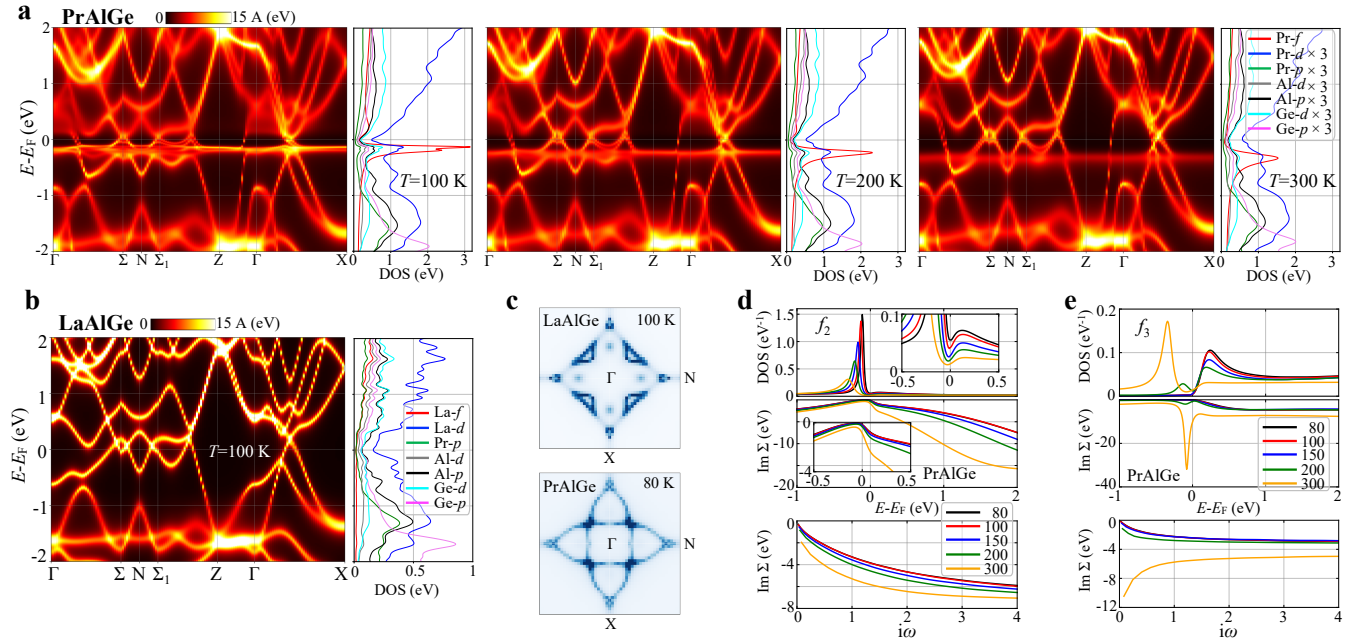


FIG. 3. **Effect of temperature on the electronic structure of PrAlGe and LaAlGe.** **a**, Calculated spectral functions and orbital projected density of states of PrAlGe at simulation temperatures of 100, 200, 300 K. **b**, Calculated spectral functions and orbital projected density of states of LaAlGe at simulation temperatures of 100 K. **c**, Fermi surfaces of LaAlGe and PrAlGe. **d**, f_2 and **e**, f_3 projected density of states, imaginary part of self-energies on the real frequency axis, and on the imaginary frequency axis. The temperature unit is Kelvin. In **(d)**, the inset shows magnified views of DOS and self-energy in the vicinity of the Fermi level.

Due to the effective Coulomb repulsion, a captivating phenomenon is observed in f_3 , which bypasses E_F by lowering the temperature. At 300 K, the imaginary part of the self-energy on the imaginary frequency axis exhibits a singularity, as shown in Fig. 3e. This implies that the f_3 at high temperatures is governed by Mott-like physics, resulting in a divergent peak of the self-energy on the real frequency axis at E_F and the formation of a pseudogap in the f_3 -driven partial DOS. The f_3 exhibits a behavior akin to that of Nd-4f at elevated temperatures in NdNiO₂ [1]. Nevertheless, a distinguishing feature is that f_3 in PrAlGe at 300 K still exhibits the suppressed DOS in the vicinity of the Fermi level. At 200 K, the self-energy decreased, resulting in f_3 DOS peak towards E_F , and the occupied DOS decreased while the unoccupied DOS increased, leaving a still suppressed DOS at E_F . Below 150 K, f_3 remains unoccupied. The weight of f_3 was redistributed to other partially occupied f orbitals, as shown in Table I.

Conclusion. The classification of strongly correlated quantum materials has been characterized by a diverse array of self-energy phenomena, stemming from a multitude of physical principles. These encompass Mott, Hund [29], and Kondo [30] physics, all of which are governed by the interplay of Coulomb and exchange interactions, as well as the localization of correlated electrons. In the context of topological and Weyl semimetals featuring rare-earth 4f quasiparticles, the 4f electrons are subject to significant self-energy due to the absence of screening caused by topological singular points. This results in the inhibition of 4f quasiparticle formation when these singular points coincide with the Fermi level. These findings suggest that these topological singular points

play a dominant role in low-energy excitations, with minimal interference from 4f quasiparticles. These results should be useful in designing topological superconductors and quantum computing devices in strongly correlated systems.

ACKNOWLEDGMENTS

We acknowledge the High Performance Computing Center (HPCC) at Texas Tech University for providing computational resources that have contributed to the research results reported within this paper. M.K. and Z.B. acknowledge the support from the National Science Foundation (Grant No. NSF DMR-2317013). C.H. Park acknowledges the support by the National Research Foundation of Korea (NRF) grant (Grant No. NRF-2022R1A2C1005548).

Competing Interests The authors declare no competing interests.

Data availability The data that support the findings of this study are available from the corresponding authors upon reasonable request.

Author contributions B.K. designed the project. B.K. performed the LQSGW+DMFT calculations and conducted the data analysis. All authors wrote the manuscript, discussed the results, and commented on the paper.

- [1] B. Kang, H. Kim, Q. Zhu, and C. H. Park, Impact of f - d Kondo cloud on superconductivity of nickelates, *Cell Rep. Phys. Sci.* **4**, 101325 (2023).
- [2] Z. Wu, Y. Fang, H. Su, W. Xie, P. Li, Y. Wu, Y. Huang, D. Shen, B. Thiagarajan, J. Adell, *et al.*, Revealing the Heavy Quasiparticles in the Heavy-Fermion Superconductor CeCu₂Si₂, *Phys. Rev. Lett.* **127**, 067002 (2021).
- [3] S. Saha, H. Sugawara, T. Namiki, Y. Aoki, and H. Sato, Anomalous properties in the low-carrier ordered phase of PrRu₄P₁₂: Consequence of hybridization between conduction and Pr $4f$ electrons, *Phys. Rev. B* **80**, 014433 (2009).
- [4] G. Chang, B. Singh, S.-Y. Xu, G. Bian, S.-M. Huang, C.-H. Hsu, I. Belopolski, N. Alidoust, D. S. Sanchez, H. Zheng, *et al.*, Magnetic and noncentrosymmetric Weyl fermion semimetals in the R AlGe family of compounds (R= rare earth), *Phys. Rev. B* **97**, 041104 (2018).
- [5] D. Tay, T. Shang, P. Puphal, E. Pomjakushina, H.-R. Ott, and T. Shiroka, Unusual ²⁷Al NMR shift in the Weyl-fermion systems LaAlGe and PrAlGe, *Phys. Rev. B* **102**, 241109 (2020).
- [6] S.-Y. Xu, N. Alidoust, G. Chang, H. Lu, B. Singh, I. Belopolski, D. S. Sanchez, X. Zhang, G. Bian, H. Zheng, *et al.*, Discovery of Lorentz-violating type II Weyl fermions in LaAlGe, *Sci. Adv.* **3**, e1603266 (2017).
- [7] H.-Y. Yang, B. Singh, B. Lu, C.-Y. Huang, F. Bahrami, W.-C. Chiu, D. Graf, S.-M. Huang, B. Wang, H. Lin, *et al.*, Transition from intrinsic to extrinsic anomalous Hall effect in the ferromagnetic Weyl semimetal PrAlGe_{1-x}Si_x, *APL Mater.* **8** (2020).
- [8] P. Puphal, V. Pomjakushin, N. Kanazawa, V. Ukleev, D. J. Gawryluk, J. Ma, M. Naamneh, N. C. Plumb, L. Keller, R. Cubitt, *et al.*, Topological magnetic phase in the candidate Weyl semimetal CeAlGe, *Phys. Rev. Lett.* **124**, 017202 (2020).
- [9] T. Wang, Y. Guo, C. Wang, and S. Yang, Correlation between non-centrosymmetric structure and magnetic properties in Weyl semimetal NdAlGe, *Solid State Commun.* **321**, 114041 (2020).
- [10] Z. Hu, Q. Du, Y. Liu, D. Graf, and C. Petrovic, High Fermi velocities and small cyclotron masses in LaAlGe, *Appl. Phys. Lett.* **117** (2020).
- [11] R. Yang, M. Corasaniti, C.-C. Le, C. Yue, Z. Hu, J.-P. Hu, C. Petrovic, and L. Degiorgi, Charge dynamics of a noncentrosymmetric magnetic Weyl semimetal, *npj Quantum Mater.* **7**, 101 (2022).
- [12] D. S. Sanchez, G. Chang, I. Belopolski, H. Lu, J.-X. Yin, N. Alidoust, X. Xu, T. A. Cochran, X. Zhang, Y. Bian, *et al.*, Observation of Weyl fermions in a magnetic noncentrosymmetric crystal, *Nat. Commun.* **11**, 3356 (2020).
- [13] I. K. Kim, B. Kang, H. Kim, and M. Choi, Crystallographic defects in Weyl semimetal LaAlGe, arXiv preprint arXiv:2401.04927 (2024).
- [14] Y. Nakajima, R. Hu, K. Kirshenbaum, A. Hughes, P. Syers, X. Wang, K. Wang, R. Wang, S. R. Saha, D. Pratt, *et al.*, Topological RPdBi half-Heusler semimetals: A new family of noncentrosymmetric magnetic superconductors, *Sci. Adv.* **1**, e1500242 (2015).
- [15] C. Shekhar, N. Kumar, V. Grinenko, S. Singh, R. Sarkar, H. Luetkens, S.-C. Wu, Y. Zhang, A. C. Komarek, E. Kampert, *et al.*, Anomalous hall effect in weyl semimetal half-heusler compounds RPtBi (R= Gd and Nd), *PNAS* **115**, 9140 (2018).
- [16] J. Chen, X. Xu, H. Li, T. Guo, B. Ding, P. Chen, H. Zhang, X. Xi, and W. Wang, Large anomalous Hall angle accompanying the sign change of anomalous Hall conductance in the topological half-Heusler compound HoPtBi, *Phys. Rev. B* **103**, 144425 (2021).
- [17] S. Dzsaber, X. Yan, M. Taupin, G. Eguchi, A. Prokofiev, T. Shiroka, P. Blaha, O. Rubel, S. E. Grefe, H.-H. Lai, *et al.*, Giant spontaneous Hall effect in a nonmagnetic Weyl-Kondo semimetal, *PNAS* **118**, e2013386118 (2021).
- [18] S. Dzsaber, D. A. Zocco, A. McCollam, F. Weickert, R. McDonald, M. Taupin, G. Eguchi, X. Yan, A. Prokofiev, L. M. Tang, *et al.*, Control of electronic topology in a strongly correlated electron system, *Nat. Commun.* **13**, 5729 (2022).
- [19] H. Siddiquee, C. Broyles, E. Kotta, S. Liu, S. Peng, T. Kong, B. Kang, Q. Zhu, Y. Lee, L. Ke, *et al.*, Breakdown of the scaling relation of anomalous Hall effect in Kondo lattice ferromagnet USbTe, *Nat. Commun.* **14**, 527 (2023).
- [20] J. Zhao, P. Mai, B. Bradlyn, and P. Phillips, Failure of topological invariants in strongly correlated matter, *Phys. Rev. Lett.* **131**, 106601 (2023).
- [21] S. Choi, P. Semon, B. Kang, A. Kutepov, and G. Kotliar, ComDMFT: A massively parallel computer package for the electronic structure of correlated-electron systems, *Comput. Phys. Commun.* **244**, 277 (2019).
- [22] C. Marianetti, K. Haule, G. Kotliar, and M. Fluss, Electronic coherence in δ -Pu: A dynamical mean-field theory study, *Phys. Rev. Lett.* **101**, 056403 (2008).
- [23] B. Kang, Y. Lee, L. Ke, H. Kim, and M.-H. Kim, Dual nature of magnetism driven by momentum dependent f - d Kondo hybridization, arXiv preprint arXiv:2305.08003 (2023).
- [24] A. Belozеров, A. Katanin, and V. Anisimov, Transition from Pauli paramagnetism to Curie-Weiss behavior in vanadium, *Phys. Rev. B* **107**, 035116 (2023).
- [25] B. Kang and S. Choi, The nature of the two-peak structure in NiO valence band photoemission, arXiv preprint arXiv:1908.05643 (2019).
- [26] B. Kang, M. Kim, C. H. Park, and A. Janotti, Mott transition and abnormal instability of electronic structure in FeSe, arXiv preprint arXiv:2310.15260 (2023).
- [27] M. Casula, P. Werner, L. Vaugier, F. Aryasetiawan, T. Miyake, A. Millis, and S. Biermann, Low-energy models for correlated materials: bandwidth renormalization from coulombic screening, *Phys. Rev. Lett.* **109**, 126408 (2012).
- [28] K. Haule, T. Birol, and G. Kotliar, Covalency in transition-metal oxides within all-electron dynamical mean-field theory, *Phys. Rev. B* **90**, 075136 (2014).
- [29] B. Kang, C. Melnick, P. Semon, S. Ryee, M. J. Han, G. Kotliar, and S. Choi, Infinite-layer nickelates as Ni-eg Hund's metals, *npj Quantum Mater.* **8**, 35 (2023).
- [30] B. Kang, S. Choi, and H. Kim, Orbital selective Kondo effect in heavy fermion superconductor UTe₂, *npj Quantum Mater.* **7**, 64 (2022).